MAGNETIC ANALYSIS OF A SINGLE-APERTURE 11 T Nb_3Sn DEMONSTRATOR DIPOLE FOR LHC UPGRADES*

B. Auchmann#, M. Karppinen, CERN, CH-1211 Geneva 23, Switzerland
V.V. Kashikhin, A.V. Zlobin, Fermilab, Batavia, IL 60510, U.S.A.

Abstract

FNAL and CERN are developing a 5.5 m long twin-aperture Nb_3Sn dipole prototype suitable for installation in the LHC. The first step of this program is the development of a 2 m long single-aperture demonstrator dipole with a nominal field of 11 T at the LHC nominal current of 11.85 kA in a 60 mm bore with 20% margin. This paper presents the results of magnetic analysis of the Nb_3Sn demonstrator dipole for the LHC upgrade.

INTRODUCTION

The planned upgrade of the LHC collimation system foresees additional collimators to be installed in the dispersion suppressor areas around points 2, 3 and 7 and around high luminosity interaction regions [1]. Replacing some 8.33 T 15 m long Nb-Ti LHC main dipole magnets (MB) with shorter 11 T Nb_3Sn dipoles compatible with the LHC lattice and main systems could provide the required space for the collimators. These twin-aperture dipoles operating at 1.9 K and powered in series with the main dipoles would deliver the same integrated strength of 119 Tm at the nominal current of 11.85 kA.

To demonstrate feasibility of this approach, CERN and FNAL have started a joint program to build a 5.5 m long twin-aperture Nb_3Sn dipole for the collimation system upgrade [2]. The first phase of this program is the design and construction of a 2 m long single-aperture demonstrator magnet with a 60 mm bore, an 11 T field at the LHC nominal current of 11.85 kA and 20% margin.

This paper presents the results of magnetic analysis of the single-aperture Nb_3Sn demonstrator including geometrical, coil magnetization and iron saturation effects. Possibilities of field quality correction at low fields using passive correction schemes are explored.

MAGNET DESIGN

The details of the single-aperture demonstrator conceptual design are reported in [2, 3]. The coil cross-section was optimized in the double-aperture LHC iron yoke with separate collared coils and a 30-mm coil-yoke gap to provide a dipole field above 11 T at 11.85 kA with ~20% margin on the load line at 1.9 K and the low-order field errors below the 10^{-4} level. The coil end spacers were optimized to minimize the integrated low-order field harmonics. The coil consists of 56 turns, 22 in the inner layer and 34 in the outer layer. The cable layer jump is integrated into the first end spacer of the coil lead end.

* Work supported by Fermi Research Alliance, LLC, under contract No. DE-AC02-07CH11359 with the U.S. Department of Energy and European Commission under FP7 project HiLumi LHC, GA no.284404
# Bernhard.Auchmann@cern.ch

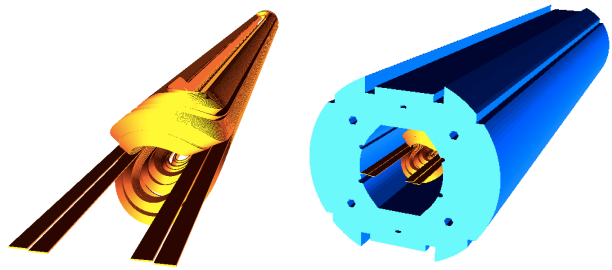

Figure 1: 3D model of the coil with the layer-jump, block transitions and coil leads (left), and the yoke (right).

Both layers are wound from a single length of 40-strand keystoned Rutherford cable [4] insulated with two layers of 0.075 mm thick and 12.7 mm wide E-glass tape. The cable is 14.7 mm wide and 1.25 mm (average) thick. The cable is made of Nb_3Sn RRP-108/127 strand 0.7 mm in diameter [5]. The strand nominal critical current density J_c(12 T,4.2 K) is 2750 A/mm^2, the effective filament size D_{eff} is 55 µm and the nominal Cu fraction is 53%.

Two coils surrounded by the multi-layer Kapton insulation and 316L stainless steel protection shells are placed inside the laminated collars made of Nirosta High-Mn stainless steel. The collared coil is installed inside the vertically split 400 mm outer diameter yoke made of 1045 iron and fixed with Aluminium clamps. The 12 mm thick 304L stainless steel shell is pre-tensioned to provide final coil pre-compression up to the maximum design field of 12 T. Two 50 mm thick 304L stainless steel end plates welded to the shell restrict the axial coil motion. The coil length is 1968±3 mm. The yoke length is 1950 mm which covers the entire coil and the Nb_3Sn/Nb-Ti lead splices. The details of magnet fabrication and magnet parameters are reported in [6].

MAGNETIC ANALYSIS

The demonstrator magnet was modeled with ROXIE [7] using properties of key structural materials. The 3D models of the 11 T demonstrator dipole coil and the iron yoke are shown in Fig. 1. Relative harmonic coefficients are given in units 10^{-4} for a reference radius of R_{ref}=17 mm.

Magnet Geometry and Iron Saturation Effect

Fig. 2 shows a 2D simulation of the transfer function $TF=B_1/I$ and the sextupole b_3 and decapole b_5 field harmonics in the current cycle due to iron yoke saturation for the 1045 iron. The persistent current effect is not considered. In the current cycle from injection to the nominal current TF reduces by 8%, b_3 reaches its maximum of 1.4 units at ~5 kA, and b_5 reduces by 30%.

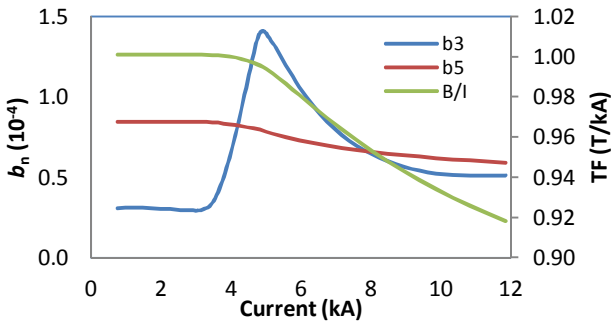

Figure 2: 2D simulation of the b_3 and b_5 (left axis) and *TF* (right axis) variations due to iron saturation.

The *TF*, b_3 and b_5 variations along the magnet are shown in Fig. 3. The b_3 and b_5 amplitude in magnet ends is quite large, reaching 300 and 250 units respectively. Nevertheless, due to the end block position optimization both return and lead ends are rather well balanced. The impact of the current leads, block connections and layer jump is visible on the lead end side.

Due to the extension of the iron yoke over the entire coil length, peak field enhancement in the coil ends reaches 0.3 T and, hence, reduces the margin on the load line by 1.9%. It also increases the magnetic length by 3.5 cm, and the b_3 component by 1.6 units.

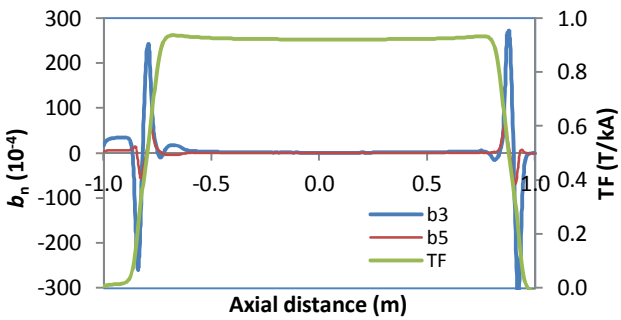

Figure 3: *TF*, b_3 and b_5 variations along the magnet.

Persistent Current Effect

The strand magnetization data were parameterized using the experimental $J_c(B)$ dependence and D_{eff}=55 µm for the RRP-108/127 strand used in the demonstrator dipole and D_{eff}=45 for the R&D RRP-150/169 strand being developed for accelerator magnets [8].

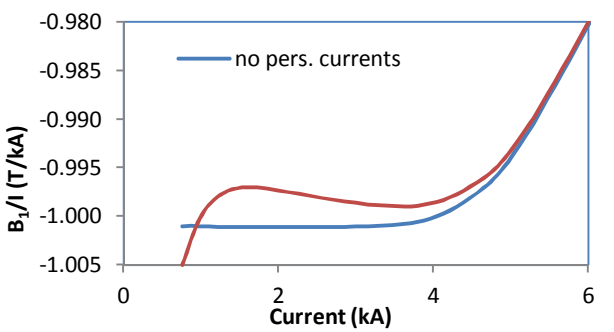

Figure 4: 2D simulation of the transfer function with and without persistent current effects.

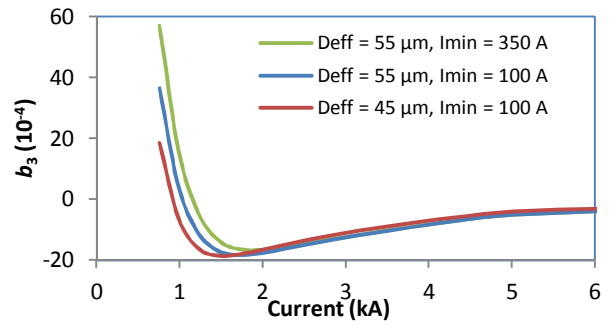

Figure 5: b_3 variation vs. magnet current for different D_{eff} and pre-cycle reset currents.

The transfer functions calculated with and without the persistent current effect for the nominal RRP-108/127 strand are compared in Fig. 4. It is clearly visible that the re-magnetization is not complete at injection level. The coil magnetization effect is smaller than the iron saturation and is visible only up to 6 kA or half of the I_{nom}.

Fig. 5 shows the dependence of b_3 induced by persistent currents in Nb_3Sn sub-elements for the RRP-108/127 and RRP-50/169 strands on magnet current with the pre-cycle reset current of 350 and 100 A. The smaller D_{eff} by a factor of 1.22 reduces b_3 at injection by a factor of 1.95. Between 1 kA and 1.7 kA the smaller filament size produces even larger $|b_3|$. Only at currents above 4.5 kA the b_3 does scale linearly with the sub-element size. It is also shown in Fig. 5 that the present LHC pre-cycle with I_{min}=100 A significantly reduces the b_3 at injection with respect to the nominal I_{min}=350 A [9].

Magnetic Calculation Summary

Table 1 summarizes the results of 2D and 3D simulation for the magnet transfer function *TF* and low order field harmonics including a_1, b_3, b_5, b_7 and b_9 at the injection and nominal currents after an LHC pre-cycle with a reset current of I_{min}=100 A. Differences between 2D and 3D results (2nd and 3rd columns) are essentially due to asymmetries on the coil lead end side.

Due to large iron saturation in the single-aperture magnet with 400 mm yoke outer diameter, the bore field B_1 at I_{nom}=11.85 kA is 10.88 T for the 1045 iron yoke. However, in the twin-aperture dipole with the iron used in MB dipoles, B_1 is 11.21 T due to the field enhancement in the twin-aperture configuration [10].

Table 1: 2D and 3D *TF* and Low-Order Field Harmonics

Parameter	Values				
Model	2D	2D	3D	2D	2D
Current	I_{inj}	I_{nom}	I_{nom}	I_{inj}	I_{nom}
Iron satur.	yes	yes	yes	yes	yes
Pers. Curr.	no	no	no	yes	yes
B_1/I, T/kA	-1.00	-0.92	-0.92	-1.01	-0.92
b_3	0.3	0.5	5.7	36.5	-1.4
b_5	0.8	0.6	1.2	7.9	0.5
b_7	-0.1	-0.1	0.0	-0.4	-0.1
b_9	0.9	1.0	0.8	1.4	1.0
a_1	0.0	0.0	3.3	0.0	0.0

ISBN 978-3-95450-115-1

Field Quality Correction

The quantitative prediction of field harmonics at injection is affected by a large level of uncertainty. Nevertheless, we can explore possibilities to correct field errors at injection, knowing that the model will be gauged to measurements at a later stage. The goal of the correction, according to beam dynamics simulations, is to keep the value of b_3 within ±20 units at low currents.

A reduction of the coil magnetization effect could be achieved by a passive correction based on superconducting strands [11] or magnetic shims [12] or their combination. An example of a passive correction scheme based on two rows of 0.8 mm Nb_3Sn strands with D_{eff}=75 μm in four sectors of 45 degrees and four 0.5 mm thick iron strips placed near the magnet midplane is shown in Fig. 6. The uncorrected and corrected b_6 for the baseline conductor RRP-108/127 are shown in Fig. 7. The effect on b_5 and higher order harmonics is small. The ferromagnetic shims are modeled using the coupling of finite elements and boundary elements. The coupled effect of ferromagnetic shims and passive strands was computed by weak coupling via iteration.

At injection current the strand magnetization in the passive strands is near zero, thus, an effective compensation is only achieved beyond the injection level. The ferromagnetic shims are used to reduce the sextupole field at injection. The described passive corrector reduces b_3 at injection from +37 to +7 units or by a factor of 5. At high currents, both the strand and shim-based compensation are diminished. The price that is paid for this compensation is a 4 mm reduction of the magnet aperture.

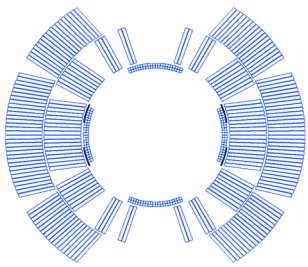

Figure 6: Passive correction by four sectors of passive strands and 0.5 mm thick ferromagnetic shims covering 15 degrees each.

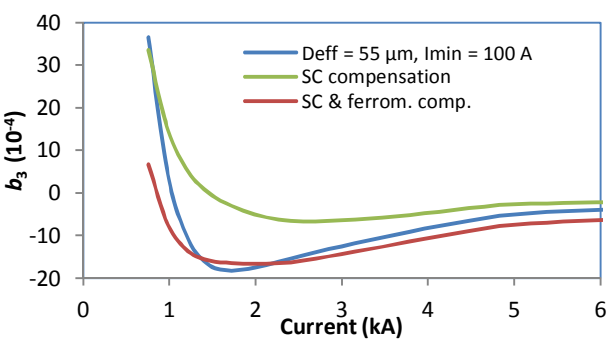

Figure 7: Sextupole correction using superconducting strands and ferromagnetic shims.

CONCLUSIONS

2D and 3D magnetic analysis has been performed for the 2 m long single-aperture demonstrator dipole including geometrical, coil magnetization and iron saturation effects. Geometrical field errors in the coil body are small due to coil cross-section optimization. The coil leads and the layer jump increase the integrated b_3 to 6 units. The iron saturation effect reduces the TF by 8%. The effect on low-order field harmonics is small.

The coil magnetization effect is relatively large at the LHC injection level due to the high J_c and large D_{eff} of the state-of-the-art Nb_3Sn strands used in the demonstrator magnet. This effect could be reduced by using strands with smaller D_{eff} and by using passive correction schemes. A short model magnet with RRP-150/169 strand and passive corrector models will be tested later this year.

REFERENCES

[1] L. Bottura et al., "Advanced Accelerator Magnets for Upgrading the LHC", IEEE Trans. on Applied Supercond., 2012.

[2] A.V. Zlobin et al., "Development of Nb_3Sn 11T Single Aperture Demonstrator Dipole for LHC Upgrades", Proc. of PAC'2011, NYC, 2011, p. 1460.

[3] A.V. Zlobin et al., "Design and Fabrication of a Single-Aperture 11T Nb_3Sn Dipole Model for LHC Upgrades", IEEE Trans. on Applied Supercond., 2012.

[4] E. Barzi et al., "Development and Fabrication of Nb_3Sn Rutherford Cable for the 11 T DS Dipole Demonstration Model", IEEE Trans. on Applied Supercond., 2012.

[5] M.B. Field et al., "Internal Tin Nb_3Sn Conductors for Particle Accelerator and Fusion Applications," Adv. Cryo. Engr. 54 (2008) 237.

[6] A.V. Zlobin et al., "Status of a Single-Aperture 11 T Nb_3Sn Demonstrator Dipole for LHC Upgrades", this conference.

[7] ROXIE, http://cern.ch/roxie

[8] E. Barzi et al., "Studies of Nb_3Sn Strands Based on the Restacked-Rod Process for High-field Accelerator Magnets", IEEE Trans. on Applied Supercond., 2012.

[9] N. Sammut et al., "Mathematical formulation to predict the harmonics of the superconducting large hadron collider magnets: III. precycle ramp rate effects and magnet characterization." Phys. Rev. Spec. Top. Accel. Beams 12 (2009).

[10] M. Karppinen et al., "Design of 11 T Twin-Aperture Nb_3Sn Dipole Demonstrator Magnet for LHC Upgrades", IEEE Trans. on Applied Supercond., 2012.

[11] M.A. Green, "Control of the Fields Due to Superconductor Magnetization in the SSC Magnets", IEEE Trans. on Magnetics23(2), (1987) 506.

[12] V.V. Kashikhin and A.V. Zlobin, "Correction of the Persistent Current Effect in Nb_3Sn Dipole Magnets", IEEE Trans. on Applied Supercond. 11(1), (2001) 2058.